Possible s^{\pm} -wave pairing evidenced by midgap surface bound states in Fe-pnictide superconductors

C. S. Liu

College of Science, Yanshan University, Qinhuangdao 066004, China

J. Y. Chang

Department of Physics, Yanshan University, Qinhuangdao 066004, China

W. C. Wu

Department of Physics, National Taiwan Normal University, Taipei 11677, Taiwan

Chung-Yu Mou

Department of Physics, National Tsing Hua University, Hsinchu 30013, Taiwan Institute of Physics, Academia Sinica, Nankang 11529, Taiwan Physics Division, National Center for Theoretical Sciences, P.O.Box 2-131, Hsinchu, Taiwan

Abstract. A phenomenological theory of tunneling spectroscopy for Fe-pnictide superconductors is developed by taking into consideration of asymmetric interface scattering between particle and holes. It is shown that in consistent with anti-phase s^{\pm} -wave pairing, appreciable zero-energy surface bound states exist on the [100] surface of Fe-pnictide superconductors. However, in contrast to the [110] bound states in d-wave cuprate superconductors, these bound states arise as a result of non-conservation of momentum perpendicular to the interface for tunneling electrons and the s^{\pm} pairing, and hence they can only exist in a small window ($\sim \pm 6^{\circ}$) in the orientation of edges near [100] direction. Our results explain why zero-bias conductance peak is often observed in tunneling spectroscopy and when it disappears, two coherent peaks show up. These results provide unambiguous signals to test the possible s^{\pm} -wave pairing in Fe-pnictide superconductors.

PACS numbers: 74.20.Rp, 74.45.+c, 74.50.+r

1. Introduction

High temperature superconductivity has been recently observed in several classes of Feprictide materials[1]. One of the key issues towards understanding the superconductivity in these systems lies in identifying the pairing symmetry of the Cooper pairs. However, up to now, gap symmetries obtained from experimental observations show remarkable dependence on material classes and doping levels[2, 3, 4] and a conclusive determination of the pairing symmetry remains unsettled. Among various candidates, the most natural and promising pairing state is considered to be the s^{\pm} -wave in which the superconducting (SC) gap exhibits a sign reversal between α and β bands and can be naturally explained by the spin fluctuation mechanism[5, 6, 7, 8, 9].

Experimentally, point-contact Andreev-reflection spectroscopy (PCARS) is considered as one of the high-resolution phase-sensitive probes for detecting the SC pairing state. For instance, zero-bias conductance peak (ZBCP) associated with the Andreev bound states (ABS) has given a direct evidence on the d-wave pairing of high- T_c cuprate superconductors [10, 11, 12, 13, 14]. However, PCARS measurements have not yielded consistent results on Fe-based superconductors. While some PCARS measurements showed two coherent peaks and indicate that SC pairing state might be fully gaped on the Fermi surface (FS)[15, 16, 17], there are also measurements showing the existence of ZBCP and implying the presence of zero-energy bound states or ABS on the interface[18, 19, 20]. More intriguingly, depending on the direction of the sample interface, some PCARS measurements exhibit the coexistence of ZBCP with finite-energy coherent peaks[21, 22].

On the theoretical side, no consensus has yet been reached to understand the PCARS data either. Although it is commonly believed that surface bound states (midgap states) are responsible for the complex PCARS, so far most theoretical studies favor that, in contrast to d-wave ABS of zero energy, surface bound states have finite energies for iron pnictides [23]. Furthermore, these surface bound states are generally resulted from the inter-band coupling that , the ways of coupling are complicated in the anti-phase s^{\pm} -wave pairing system.

Among many theoretical works, the study in Ref. [24] believes the coupling are from the boundary. The matching condition for the wave function at the interface is used to produce two-band coupling on the basis of an extension of quantum waveguide theory. Based on the Green's function formulation in this study, the differential conductance curves versus bias voltage explicitly support the emergence of ABS as a manifestation of interference effects between the bands. The other study, however, suggests that the coupling is due to the direct coupling of two-orbital coupling[25]. In these models, ABS was also found to appear at surface due to the sign change in the gap function when taking the inter-band quasi-particle (QP) scattering into account. Inspired by the tunneling magnetoresistance where the leads are usually transition metals with multiband d orbitals, a new type of two-band coupling is set up, in which it is assumed that when an electron crosses the interface from the lead to the Fe-based superconductors, it

tunnels into the first or second band on the right with the ratio of probability amplitudes $\alpha_0[26]$. It was found that Andreev bound states can appear at both nonzero and near zero energies by changing values of α_0 .

To address these puzzling issues and account for the observed ZBCP, in this paper, we propose a different coupling scheme of two orbitals in the s^{\pm} -wave pairing state by considering asymmetric interface scatterings between particles and holes. Theoretically, the interface scatterings for quasi-particles and quasi-holes of the same band are generally different due to that there is no particle-hole symmetry in the normal metal side. Asymmetry in the probability amplitude of two orbitals would induce asymmetry between particles and holes in the same orbital. By assuming asymmetry between particles and holes in each orbital, we extend the Blonder-Tinkham-Klapwijk (BTK) formalism [27] to investigate the differential conductance of the junction between a normal metal and a Fe-pnictide superconductor. It is shown that by including directional dependence of QPs interplaying between different bands, ZBCP emerges in the presence of asymmetry between particles and holes. The existence of the surface bound state is due to the anti-phase s^{\pm} -wave pairing potentials of different bands and the orientation in terms of multi-band FS topology. Our results are consistent with recent PCARS measurements (with zero energy or nonzero energy) in iron-pnictide superconductors. In particular, it is shown that ZBCP is sensitive to surface orientation. Off the [100] direction, the zero-bias peak disappears and is replaced by two coherent peaks. These features provide unambiguous signals to test the possible s^{\pm} -wave pairing in Fe-prictide superconductors.

The paper is organized as follows. In Sec. 2, we present the model and basic formalism for studying the tunneling conditions. This formalism is based on the WKBJ approximation of the Bogoliubov-de Gennes (BdG) equations and consider QPs interplaying between different bands. In Sec. 3, we fist give the numerical solutions in Sec. 3.1 and then illustrate in Sec. 3.2 the ZBCP existing due to a close Saint-James cycle in the s^{\pm} pairing of two bands. At last in Sec. 3.3, conductance spectrum were computed and compared to the existing experimental data. In particular, we show how the ZBCP can exist in a small window ($\sim \pm 6^{\circ}$) in the orientation of edges near [100] direction and how the coherent peaks can be observed in nonzero-energy in some case. A brief summary is given in Sec. 4.

2. Model and Method

In contrast to cuprates whose low-energy electronic structure is dominated by Cu $3d_{x^2-y^2}$ orbital, the electronic structure of Fe-based compounds involves all five Fe 3d orbitals forming multiple FS sheets. The FS topology and gap opening are observed to be slightly different between different material classes and compositions. Taking the newly found $Tl_{0.58}Rb_{0.42}Fe_{1.72}Se_2$ and $K_{0.8}Fe_{1.7}Se_2$ samples for example, high-resolution ARPES measurements have found that FS for $Tl_{0.58}Rb_{0.42}Fe_{1.72}Se_2$ consists of two electron-like FS sheets around the Γ point[28]. The FS around the M point shows

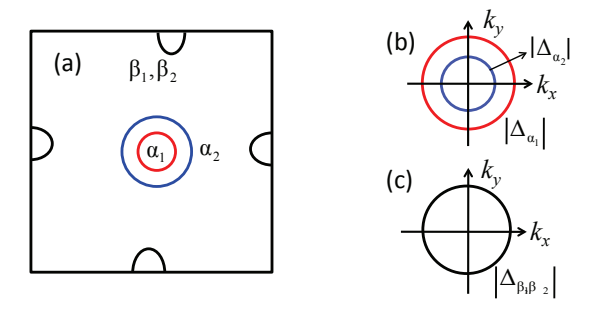


Figure 1. (Color online) Panel (a): schematic plot of the Fermi surfaces of two band in unfolded Brillouin zone. Panel (b) & (c) plot the pairing amplitudes for α and β band respectively.

a nearly isotropic SC gap of ~ 12 meV. The large FS near the Γ point also shows a nearly isotropic SC gap of ~ 15 meV, while there is no clear SC gap opening for the inner tiny FS. On the other hand, for $K_{0.8}Fe_{1.7}Se_2$, a nearly circular FS is formed around M point[29]. The absence of a hole-like FS is because hole-like band is shifted down below the Fermi energy. The FS and SC gap properties of $Tl_{0.58}Rb_{0.42}Fe_{1.72}Se_2$ and $K_{0.8}Fe_{1.7}Se_2$ are quite different from those of the earlier found sample $Ba_xK_{1-x}Fe_2As_2$, including all under-, optimally- and over-doped regimes [30, 31, 32, 33, 34]. For $Ba_xK_{1-x}Fe_2As_2$, two large circular FSs are found on the Γ point and one little FS on the M point. The SC gap on each FS is nearly isotropic and the gap value on each FS nearly scales with T_c over a wide doping range $(0.25 \le x \le 0.7)$.

To simplify discussions and capture the key elements, we use the following model for Fe-pnictide superconductors. The so-called α_1 and α_2 Fermi sheets are concentric and nearly circular hole pockets around the Γ point. While β_1 and β_2 Fermi sheets are nearly circular electron pockets around the M points. SC gap is isotropic on each FS but with different amplitude. For s^{\pm} -wave symmetry, gaps on α and β bands have a sign reversal and the corresponding magnitudes will be denoted by Δ_{α} and Δ_{β} . Our discussions will follow the above picture of FSs and SC gap structures, as sketched in Fig. 1. As it will be shown, slight distortion of the FS will not affect much the results.

We first consider a Fe-pnictide bulk superconductor with a perfectly flat and infinitely large interface located at x = 0. The superconductor occupies x > 0. For each band, QP states have a coupled electron-hole character and can be described by the BdG equations [35]

$$\begin{bmatrix} \hat{\xi} & \Delta(\mathbf{r}) \\ \Delta^*(\mathbf{r}) & -\hat{\xi} \end{bmatrix} \begin{bmatrix} u(\mathbf{r}) \\ v(\mathbf{r}) \end{bmatrix} = E \begin{bmatrix} u(\mathbf{r}) \\ v(\mathbf{r}) \end{bmatrix}, \tag{1}$$

where $\Delta = \Delta_{\alpha}$ or Δ_{β} , E is the total energy of the quasi-particle, $\hat{\xi} \equiv -\hbar^2 \nabla^2/2m - \mu$ with μ being the chemical potential potential, and m the electron mass. Within the

Possible s^{\pm} -wave pairing evidenced by midgap surface bound states in Fe-pnictide superconductors 5

WKBJ approximation[36], one seeks solutions of the form

$$u(\mathbf{r}) = e^{i\mathbf{k}_F \cdot \mathbf{r}} \eta(\mathbf{r}) \text{ and } v(\mathbf{r}) = e^{i\mathbf{k}_F \cdot \mathbf{r}} \chi(\mathbf{r}),$$
 (2)

where \mathbf{k}_F is the Fermi wavevector satisfying $\mu = \hbar^2 k_F^2/(2m)$ and in contrast to the plane-wave exponential factors, $\eta(\mathbf{r})$ and $\chi(\mathbf{r})$ are slowly varying functions. We shall neglect the difference of k_F in α and β bands and the second derivatives in Eq. (1). We then obtain the Andreev equations

$$[i\hbar (\mathbf{v}_F \cdot \nabla) + E] \eta (\mathbf{r}) + \Delta (\mathbf{r}) \chi (\mathbf{r}) = 0,$$

$$[i\hbar (\mathbf{v}_F \cdot \nabla) - E] \chi (\mathbf{r}) + \Delta (\mathbf{r}) \eta (\mathbf{r}) = 0.$$
 (3)

It is assumed that the pairing gap function takes the steplike form, $\Delta(x, y, z) = \Delta e^{i\phi}\theta(x)$ with ϕ being the SC phase. In reality, it sags a little near the interface at the distance of the mean free path or so. In the following, we neglect the above so-called proximity effect since it gives only small corrections. As the wave-vector components parallel to the interface, k_y , are conserved for all possible processes, the problem is effectively reduced to one-dimensional one.

The two (α and β) bands are assumed to be decoupled completely and thus one can proceed to obtain various reflection coefficients for each individual band. Outside of the interface (x < 0), electrons and holes, if existing, are free electrons and free holes and we denote their wave functions by

$$\psi_e^{\pm}(x) = \begin{pmatrix} 1 \\ 0 \end{pmatrix} e^{\pm ik_+ x}; \quad \psi_h^{\pm}(x) = \begin{pmatrix} 0 \\ 1 \end{pmatrix} e^{\pm ik_- x}$$
 (4)

with k_y suppressed. As is easily seen from the BdG equations, the wave vectors $k_{\pm} = k_F \sqrt{1 \pm E/\mu}$. Here e(h) denotes for electron (hole) and +(-) corresponds to movement parallel (antiparallel) to the x-axis.

Inside the superconductor, one can solve the Andreev equation (3) to obtain electron- and hole-like quasi-particle wave functions

$$\Psi_e^{\pm}(x) = \begin{pmatrix} ue^{i\phi/2} \\ ve^{-i\phi/2} \end{pmatrix} e^{\pm iq_+ x},\tag{5}$$

$$\Psi_h^{\pm}(x) = \begin{pmatrix} ve^{i\phi/2} \\ ue^{-i\phi/2} \end{pmatrix} e^{\pm iq_- x}.$$
 (6)

Here the dispersion laws and expressions for u, v also follow the BdG equations together with the condition $u^2 + v^2 = 1$. After some algebra, we obtain

$$u(E) = \sqrt{\frac{1 + \sqrt{1 - \Delta^2/E^2}}{2}},$$
 (7)

$$v(E) = \sqrt{\frac{1 - \sqrt{1 - \Delta^2/E^2}}{2}},$$
 (8)

$$q_{\pm} = k_F \sqrt{1 \pm \frac{\sqrt{E^2 - \Delta^2}}{\mu}}.$$
 (9)

Possible s^{\pm} -wave pairing evidenced by midgap surface bound states in Fe-pnictide superconductors6

For sub-gap excitations $(E < \Delta)$, u, v, and q will acquire imaginary parts. Physically possible sub-gap solutions must decay into the bulk of the superconductor. In the present case, it allows for Ψ_e^+ and Ψ_h^- only at $x \to \infty$.

To investigate the tunneling spectroscopy of a normal metal-superconductor point contact located at x=0, we consider an electron that is incident on the boundary from the normal metal side x<0. For elastic scattering, ψ_e^+ , ψ_e^- , and ψ_h^+ are 3 possible quasi-particle states at the normal metal side with the same energy. Hence the quasi-particle wave function Ψ_N at x<0 can be generally written as

$$\Psi_N = \psi_e^+ + r_{ee}\psi_e^- + r_{eh}\psi_h^+, \tag{10}$$

where r_{ee} and r_{eh} characterize two possible reflection amplitudes with r_{ee} describing the normal reflection (reflected as electrons) and r_{eh} describing the Andreev reflection (reflected as holes). On the SC side (x > 0), the quasi-particle wavefunction Ψ_C is also a superposition of electron-like (Ψ_e) and hole-like (Ψ_h) wave functions and can be generally written as

$$\Psi_S = t_{ee} \Psi_e^+ + t_{eh} \Psi_h^-, \tag{11}$$

where t_{ee} and t_{eh} are transmission amplitude for electron-like and hole-like quasiparticles. For multi-orbital superconductors, elastic scatterings near boundary generally mixes quasi-particles of different bands at the same energy. For the model we adopt for Fe-pnictide superconductors, there are 4 possible quasi-particle states in the SC side with the same energy: $\Psi_{e,\alpha}^+$, $\Psi_{e,\beta}^+$, $\Psi_{h,\alpha}^-$ and $\Psi_{h,\beta}^-$. Hence the electron-like and hole-like wave functions can be generally written as

$$\Psi_{e}^{+} = A\Psi_{e,\alpha}^{+} + B\Psi_{e,\beta}^{+}
\Psi_{h}^{-} = C\Psi_{h,\alpha}^{-} + D\Psi_{h,\beta}^{-},$$
(12)

where A, B, C, and D are amplitudes for quasi-particles and quasi-holes in α and β bands. Combining Eqs.(11) and (12), it is clear that coefficients A and D can be absorbed into t_{ee} and t_{eh} and the electron-like and hole-like wave functions can be recast into the following forms

$$\Psi_e^+ = \Psi_{e,\alpha}^+ + \gamma \Psi_{e,\beta}^+ \tag{13}$$

$$\Psi_h^- = \gamma' \Psi_{h,\alpha}^- + \Psi_{h,\beta}^-. \tag{14}$$

Here γ' (= C/D) and γ (= A/B) are two coefficients that characterize coupling of α and β bands. For bulk superconductors without boundaries, quasi-particles in α and β bands are not mixed. Hence γ and $\gamma's$ are independent parameters in this case. However, the boundary introduces definite coupling between α and β bands. Therefore, γ and $\gamma's$ are no longer independent parameters. In the simplest assumption[26], one sets $1/\gamma' = \gamma \equiv \alpha_0$. In this case, quasi-particles and quasi-holes have the same coupling ratio in α and β bands. As indicated in the introduction, the resulting Andreev bound states generally appear at finite energies and do not explain the observed ZBCP in PCARS.

Possible s^{\pm} -wave pairing evidenced by midgap surface bound states in Fe-pnictide superconductors?

In order to explain the observed ZBCP in PCARS, we first note that the boundary scatterings for quasi-particles and quasi-holes of the same band are generally different due to that there is no particle-hole symmetry in the normal metal side. The asymmetry between quasi-particles and quasi-holes is exhibited in Eqs.(13) and (14) as the factor γ' for the α band and γ for the β band. Note that there is a tendency to preserve an overall particle-hole symmetry in the superconducting side as reflected in Eqs.(13) and (14), where the asymmetry for the β band is reversed and is the ratio of the amplitude of quasi-particle to that of the quasi-hole. Physically, Eq.(13) implies that a quasi-particle in α band can scatter into β band. Since when a quasi-particle transmits from α band into β band, a hole is left in α band. Hence a quasi-particle tunneling from α band into β band is equivalent to a quasi-hole tunneling from β band into α band, which, when combined with Eq.(14), implies $\gamma' = \gamma$. Therefore, we consider a class of parameters in which

$$\gamma' = \gamma \tag{15}$$

is obeyed. In this class of parameters, a large probability amplitude for a quasi-particle tunneling from α -band to β -band will result in a large probability amplitude for a quasi-hole tunneling from β -band to α -band. As a result, unlike the phenomenological ratio of probability amplitudes $\alpha_0[26]$, asymmetry in the tunneling probability amplitude of α and β would induce asymmetry between particles and holes in the same orbital. We shall show in subsection 3.3 that the introduction of asymmetric factor γ can naturally explain experimental data.

In addition to the above consideration on mixing of α and β bands, the potential scattering near the boundary can be generally described by a delta-function barrier potential, $H\delta(x)$. Matching the wave functions and their derivatives at the interface (x=0)[27]

$$\Psi_{N}(x)|_{x=0^{-}} = \Psi_{S}(x)|_{x=0^{+}},$$

$$\frac{2mH}{\hbar^{2}}\Psi_{S}(x)|_{x=0^{+}} = \frac{d\Psi_{S}(x)}{dx}|_{x=0^{+}} - \frac{d\Psi_{N}(x)}{dx}|_{x=0^{-}},$$
(16)

yields complete solutions of all scattering amplitudes. Note that the boundary conditions imposed in Eq.(16) actually consist of four equations and represent boundary conditions directly on electron wave functions. After some tedious but straightforward derivations, we find that when $\phi_{\alpha} - \phi_{\beta} = \pi$ or 0, reflection coefficients are given by

$$\Lambda r_{eh} = (\gamma u_{\alpha} + \epsilon u_{\beta}) (v_{\alpha} + \epsilon \gamma v_{\beta}),
\Lambda r_{ee} = (iZ + Z^{2}) [(\epsilon v_{\alpha} + \gamma v_{\beta}) (\gamma v_{\alpha} + v_{\beta}) - (u_{\alpha} + \gamma u_{\beta}) (\epsilon \gamma u_{\alpha} + u_{\beta})].$$
(17)

Here $Z = 2mH/\hbar^2 k_F$, $\Lambda = (1 + Z^2)(\epsilon \gamma u_\alpha + u_\beta)(u_\alpha + \gamma u_\beta) - Z^2(\gamma v_\alpha + v_\beta)(\epsilon v_\alpha + \gamma v_\beta)$, and when $\phi_\alpha - \phi_\beta = 0$, $\epsilon = 1$; otherwise, $\epsilon = -1$. The tunneling conductance is correspondingly given by the two solved coefficients r_{ee} and r_{eh} as

$$\sigma_S = 1 + |r_{eh}|^2 - |r_{ee}|^2. \tag{18}$$

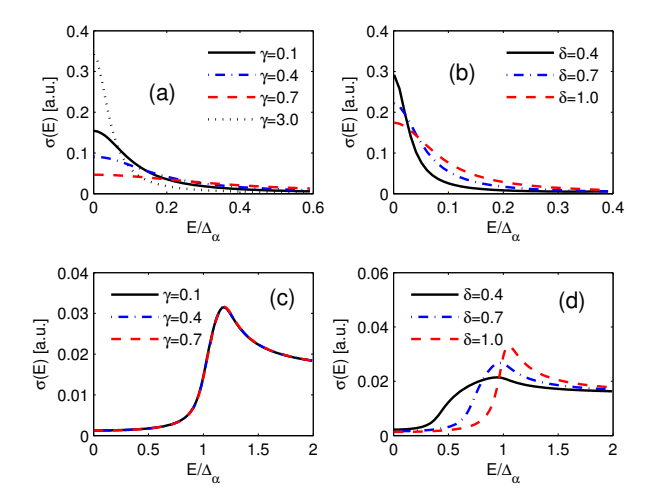


Figure 2. (Color online) Panel (a) and (b): Tunneling conductance for the pairing symmetry s^{\pm} . Panel (c) and (d): Tunneling conductance for the pairing symmetry s^{++} . Here $\delta = \Delta_{\beta}/\Delta_{\alpha}$ and k_y of the incident electron is zero. Parameters in Panel (a) and (c) are $\delta = 1.2$ and in Panel (b) and (d) are $\gamma = 0.1$. Except for (c) where we set Z = 1, Z is taken to be 8 in other cases. Note that a scattering broadening $\Gamma = 0.08$ is used to prevent divergence in all cases.

3. Results and Discussions

3.1. Numerical simulations

Fig. 2 shows the zero-temperature conductance for SC pairing s^{\pm} of two bands when k_y of the incident electron is zero. Sharp ZBCP emerges in (a) and (b) when the mixing coefficient γ is take at very small or very large values. The sharp ZBCP can be attributed to the existence of zero-energy Andreev bound states. Indeed, Eq.(17) implies that a bound state exists when

$$\Lambda = 0. \tag{19}$$

For large Z, since $\Lambda \sim Z^2\{(\epsilon \gamma u_\alpha + u_\beta)(u_\alpha + \gamma u_\beta) - (\gamma v_\alpha + v_\beta)(\epsilon v_\alpha + \gamma v_\beta)\}$, we find that in the limit of large γ , $\Lambda = -\gamma(u_\alpha u_\beta - v_\alpha v_\beta)$, while for $\gamma \to 0$, $\Lambda = (u_\alpha u_\beta - v_\alpha v_\beta)$. Because $u_\alpha u_\beta - v_\alpha v_\beta$ vanishes when E = 0, both $\gamma \to \infty$ and $\gamma \to 0$ support zero energy solution. Hence zero-energy bound state exists in these limits. When γ is not too large or non-vanishing, the zero-energy bound state is partially destructed. For comparison, we also present results for the pairing symmetry s^{++} , shown in Figs. 2 (c) and (d). Clearly, the zero-energy bound states are absent. The tunneling conductance exhibits one quasi-particle peak which indicates that the conductance is not a simple sum over two individual bands. In particular, the numerical solutions indicate that the position of quasi-particle peak is insensitive to the mixing constant γ and is sensitive to the ratio of two gap amplitudes, δ .

3.2. Quantization condition of midgap states and zero energy bound state

In order to understand the arising of ZBCP in limits of $\gamma \to 0$ and $\gamma \to \infty$, we further examine the zero energy bound state by investigating multiple scatterings of quasi-particles. The examination will generally yield the quantization condition for existence of midgap states and the condition for the existence of zero energy bound state.

For this purpose, we consider quasi-particles in a thin normal metal layer of width L attached to a Fe-pnictide superconductor as shown in Fig. (3). In the limit of $L \to 0$, as first shown by Hu[10], semi-classical quantization rule is sufficient to determine midgap states. For this purpose, we first consider quasi-particles with energy E off from a superconductor with a single band at x > 0 with gap magnitude being Δ . Following the same procedure outlined in Sec. 2, matching the wave functions and their derivatives at the interface (x = 0), one obtains the coefficients r_{eh} and r_{ee} . These coefficients can be greatly simplified under the so-called Andreev approximation. In the lowest non-vanishing order in $\max(\Delta, E)/\mu$, one can take $k_{\pm} \approx q_{\pm} \approx k_F$ and

$$k_{+} - q_{-} \approx q_{+} - k_{-} \approx k_{F} \frac{u}{v} \frac{\Delta}{2\mu}.$$
 (20)

Therefore, we find that the Andreev reflection coefficients can be approximated as [27, 37]

$$r_{eh(he)} = e^{\mp i\phi} \times \begin{cases} e^{-i\cos^{-1}\frac{E}{\Delta}}, \text{ for } E \leq \Delta, \\ e^{-\cosh^{-1}\frac{E}{\Delta}}, \text{ for } E > \Delta. \end{cases}$$
 (21)

For the sub-gap (or midgap) state, $E \leq \Delta$, we thus have for the total Andreev reflection $|r_{eh(he)}(E)|^2 = 1$ and consequently the normal reflection can be safely neglected.

When a subgap-energy electron $(E < \Delta)$ enters the interface, an Andreev hole will reflect from the interface due to the electron-hole coupling through the pairing potential Δ . Since there are two bands at x > 0, an electron can be reflected either by the α band or by the β band. Therefore, it is convenient to keep track on band origin of quasi-particles in the metal layer by writing the wavefunction $\psi(x, E)$ of quasi-particle for -L < x < 0 as

$$\psi(x, E) = a\psi_{\alpha e}^{+}(x, E) + b\psi_{\alpha h}^{+}(x, E) + c\psi_{\beta e}^{-}(x, E) + d\psi_{\beta h}^{-}(x, E) + a'\psi_{\beta e}^{+}(x, E) + b'\psi_{\beta h}^{+}(x, E) + c'\psi_{\alpha e}^{-}(x, E) + d'\psi_{\alpha h}^{-}(x, E) . (22)$$

Here a, b, c, d, a', b', c', and d' are coefficients to be determined by boundary conditions and we have set $k_y = 0$ for sake of illustration. As illustrated in Fig.3, within the metal layer, there are several possible close cycles, known as Saint-James cycles [12], that quasi-particles may form during their scatterings at x = 0 and x = -L. For instance, an α electron particle may be reflected as an α hole at x = 0 and the α hole gets specular reflection at x = -L. The specularly reflected α hole will scatter back as an α electron at x = 0 and form an intra-band close cycle. Similar intra-band close cycles also exist for the β band. Due to non-conservation of momentum perpendicular to the interface at x = 0 during scattering, there are also inter-band Saint-James cycles. As explained, the asymmetry between particles and holes due to scatterings is taken into account by γ in Eqs.(13) and (14). In the limit of $\gamma \to 0$, $\Psi_{e,\alpha}^+$ and $\Psi_{h,\beta}^-$ (equivalently, $\Psi_{h,\alpha}^+$ and

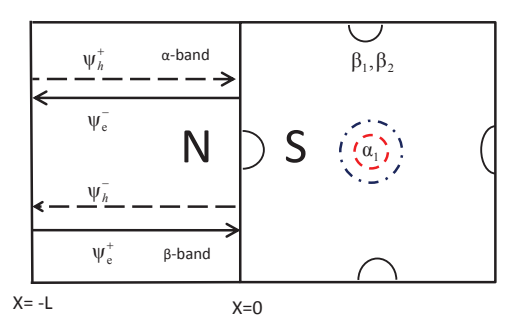


Figure 3. (Color online) Schematic representation of an Andreev-Saint-James cycle for a two-band s^{\pm} -wave superconductor coated with a normal-metal layer, the interface being oriented perpendicular to the [100] direction.

 $\Psi_{e,\beta}^{-}$) dominate in the SC side. Since quasi-particle wavefunctions are continuous across the junction x=0, solutions with vanishing a', b', c', and d' correspond to the limit of $\gamma \to 0$. Similarly, solutions with vanishing a, b, c, and d correspond to the limit of $\gamma \to \infty$.

Quantitatively, Eq.(10) implies that in each scattering, ψ_e^+ has to match $r_{eh}\psi_h^+$ and ψ_h^- has to match $r_{he}\psi_e^-$. Equivalently, ψ_e^- has to match $r_{he}\psi_h^-$ and ψ_h^+ has to match $r_{eh}\psi_e^+$. Together with the hard wall boundary condition, $\psi(-L) = 0$, applied to particles and holes separately, we find that the inter-band cycle in the limit $\gamma \to 0$ implies the following relations

$$a\psi_{\alpha e}^{+}(0,E) = r_{eh}(\alpha)b\psi_{\alpha h}^{+}(0,E),$$

$$d\psi_{\beta h}^{-}(0,E) = r_{he}(\beta)c\psi_{\beta e}^{-}(0,E),$$

$$c\psi_{\beta e}^{-}(-L,E) = -a\psi_{\alpha e}^{+}(-L,E),$$

$$b\psi_{\alpha h}^{+}(-L,E) = -d\psi_{\beta h}^{-}(-L,E),$$
(23)

where the last two equations result from the specular reflections at x = -L. Clearly, by taking $L \to 0$, Eq. (23) implies $r_{eh}(\alpha)r_{he}(\beta) = 1$. Similarly, for $\gamma \to \infty$, one replaces a, b, c, and d by a', b', c', and d'. Furthermore, α and β in (23) get exchanged. Hence we get a reversed cycle and obtain $r_{eh}(\beta)r_{he}(\alpha) = 1$. By using Eq. (21), we conclude that the midgap energy in a semi-infinite Fe-pnictide superconductor that occupy x > 0 must satisfy

$$\cos^{-1}\frac{E_n}{\Delta_\alpha} + \cos^{-1}\frac{E_n}{\Delta_\beta} = \pm (\phi_\alpha - \phi_\beta) + 2n\pi, \tag{24}$$

where $n=0, \pm 1, \pm 2, \cdots$. Eq. (24) represents one of the major results in this paper. If one identifies the scattering phase across the interface as the generalized momentum, $p_i = \pm \phi_i + \cos^{-1}\frac{E}{\Delta_i}$, Eq. (24) can be rewritten as $\sum_{i=(\alpha,\beta)} p_i = 2n\pi$, which is in consistence with the semiclassical quantization condition. When $\Delta \phi = \phi_{\alpha} - \phi_{\beta} = \pm \pi E_n < \min(\Delta_{\alpha}, \Delta_{\beta})$, Eq. (24) only supports the zero-energy solution $(E_n = 0)$. It indicates that zero-energy surface bound states can exist in the semiclassical approximation even in the limit of a zero-thickness normal slab. The zero-energy states

are formed in the normal side and extend into the superconducting side over a coherence length which is similar the case of d-wave superconductor studied by Hu[10]. Moreover the zero-energy surface bound state is only sensitive to the phase difference of the two-band pairing and has nothing to do with the paring amplitudes. It should be noted that no Saint-James cycle exists when $\Delta_{\alpha} < E_n < \Delta_{\beta}$ or $\Delta_{\alpha} < \Delta_{\beta} < E_n$ because according to Eq. (21), the currents will decay exponentially.

3.3. Comparison with the experimental data

To consider how midgap states are related to real PCARS measurements, we first note that for point-contact junctions, even though the interface of the junction is not an infinitely flat plane, the contact region is flat and is often large in comparison to the atomic scale and the BTK theory is applicable[40]. However, in contrast to planar junctions, point-contact junctions are often plagued with uncertainty in exact orientation of the junction interface. Therefore, it is crucial to include orientational dependence in the tunneling spectroscopy. For this purpose, in the following we extend the analysis to include $k_y \neq 0$.

We first note that if the pairing gaps between different FSs are extended s-wave with sign reversal, there will be four kinds of zero-energy surface bound states (or zero-energy Saint-James cycles) corresponding to various combinations of interband FSs: $\alpha_1 - \beta_1$, $\alpha_1 - \beta_2$, $\alpha_2 - \beta_1$, and $\alpha_2 - \beta_2$. As indicated in Fig. 3, zero-energy Saint-James cycles is sensitive to the direction. It can only exist when only when quasi-particles can scatter across α and β bands. The window for such scatterings can be estimated as the spanning angle of β band with respect to the $\mathbf{k} = 0$ point, which limits the orientations of interfaces to fall into a small window around $\pm 6^{\circ}$ near the [100] direction. In contrast to other pairing symmetry such as d-wave which also supports zero-energy bound states but with a large window for observing these states[14].

In addition to the above four zero-energy surface bound states, there also exist nonzero-energy surface bound states (or nonzero-energy Saint-James cycles) corresponding to various combinations of intraband FSs: $\alpha_1 - \alpha_1$, $\alpha_1 - \alpha_2$, $\alpha_2 - \alpha_2$, $\beta_1 - \beta_1$, $\beta_1 - \beta_2$ and $\beta_2 - \beta_2$. This is the key why two coherent peaks are often observed in the PCARS measurements. It has also been pointed out that nonzero ABS can exist in the s^{\pm} -wave superconductor of multi-gap nature due to interference effects[24, 26] and inter-band quasi-particle scattering[25]. These effects may determine whether an electronic trajectory crosses two bands or only one band. It may also contribute to subgap peaks in the angular dependence of conductance spectra for s^{\pm} -wave Fe-pnictide superconductors.

To realize the above analysis in real PCARS, we calculate the conductance in $\gamma \gg 1$ case. The results in $\gamma \ll 1$ case will remain unchanged. In these limits, results of the tunneling spectroscopy can be simplified. On the SC side (x>0), for a given k_y and E, since k_y is conserved, available quasiparticles depends on the magnitude of k_y . For $k_y \sim 0$, i.e., near the [100] direction as shown in Fig. 3, the transited QPs can be either on

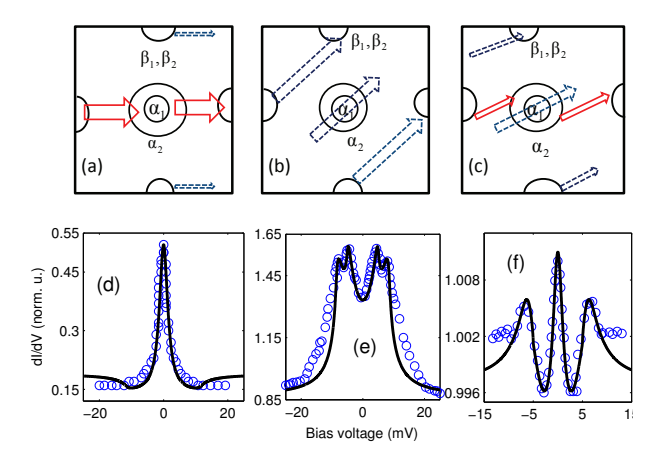


Figure 4. (Color online) Panel (a)–(c): schematic plots of different-direction electron tunneling on iron-pnictide SC interfaces. The arrows denote the electron tunneling directions and how different bands are coupled. The arrows with red sold lines show the particular directions where zero-energy Saint-James cycle can form. The weights of the arrows denote their possible contributions to the differential conductance. Panel (d)–(f): fitting to the I-V data of (d) SmFeAsO_{0.9}F_{0.1} sample ($T_c = 51.5$ K) (taken from Ref. [[18]]); (e) TbFeAsO_{0.9}F_{0.1} sample ($T_c = 50$ K) (taken from Ref. [[22]]); and (f) SmFeAsO_{0.9}F_{0.1} sample ($T_c = 51.5$ K) (taken from Ref. [[21]]).

the α band or β band, experiencing different pairing potentials for s^{\pm} -wave Fe-pnictide superconductors. This enables the completion of zero-energy Saint-James cycle. We shall set the electron-like QP wavefunction Ψ_e^+ in Eq.(11) to be in the quasi-particle wavefunction of the α band with pairing potential $\Delta_{\alpha}e^{i\phi_{\alpha}}$. Similarly, the hole-like QP wave function Ψ_h^+ in Eq.(11) is obtained by using pairing potential $\Delta_{\beta}e^{i\phi_{\beta}}$. Assuming electrons are incident with an angle θ with respect to the [100] direction, one can set $k_y = k_F \sin \theta$. By matching the wave functions and their derivatives at the interface x = 0 according to Eq.(16), the normalized tunneling conductance $\tilde{\sigma}_S$ is obtained via Eq.(18). We obtain

$$\tilde{\sigma}_S(E) = \frac{16\left(1 + \cos^2\theta \left|\Gamma_\alpha\right|^2\right)\cos^4\theta + 4Z^2\left(1 - \left|\Gamma_\alpha\Gamma_\beta\right|^2\right)\cos^2\theta}{\left|4\cos^2\theta + Z^2 - Z^2\left|\Gamma_\alpha\Gamma_\beta\right|\exp\left[i\left(\phi_\alpha - \phi_\beta\right)\right]\right|^2}.$$
 (25)

Here Γ 's are defined as $\Gamma_{\alpha,\beta} = E/|\Delta_{\alpha,\beta}| - \sqrt{(E/|\Delta_{\alpha,\beta}|)^2 - 1}$. Similar derivation of Eq. (25) can be found in Ref. [11] where a single-band system was studied.

Eq. (25) is valid only when $\theta \sim 0$ (and thus $k_y \sim 0$). In this case, as shown in Fig. 4(a), due to non-conservation of k_x , the dominant contribution to the current comes from QPs from both α and β bands. The low-energy differential conductance will thus be dominated by the zero-energy bound states that arise from the inter-band QP transitions although the nonzero-energy bound states may also have some effects on it. Thus the ZBCP found in PCARS is due to the zero-energy bound states that exist in the interface when electrons tunnel normal to the interface along the [100] direction. This is verified in Fig. 4(d), where we have simulated the PCARS data presented in

Ref. [21] by assuming that all electrons are tunneling across the interface along the [100]-direction. Eq. (25) is used to obtain the best fitting with $\Delta_{\alpha} = 8$ and $\Delta_{\beta} = 8$ under the proposed sign-reversal s^{\pm} -wave pairing. Here the integration over angles is not necessary for the small window of angles. The normalized barrier height is taken to be Z = 5 and the scattering broadening $\Gamma = 0.5$.

It should be emphasized that ZBCP is more sensitive to the phase difference than the gap amplitude and when a more realistic FS together with a more realistic extended s-wave gap are used, a much better fitting, especially in the nonzero-energy region, will be obtained. The ZBCP found here can only exist when range of k_y covers the β band. Using experimental data[33, 34], this corresponds to a small window of $\pm 6^{\circ}$ for interfaces around [100] direction.

We next consider the case of the [110] direction in Fig. 4(b) for which the interface is off the window of $\pm 6^{\circ}$ about [100]. In this case, the conservation of k_y removes QPs in the β band. Therefore, the crossing term $\Gamma_{\alpha}\Gamma_{\beta}$ in Eq. (25) is absent. Hence the denominator in Eq. (25) is always finite and it results in in the absence of the ZBCP. In this case, however, non-zero Saint-James cycles of two separate bands are important. This is similar to the point-contact conductance spectra of MgB₂, which is also a multiband superconductor and the tunneling spectrum is usually fitted by summation of two single-band tunneling probabilities[38, 39]. In Fig. 4(e), we use the two-gap s^{\pm} -wave model to fit the PCARS data reported in Ref. [22] by using Eq.(25). The best fitting was obtained with the two gap amplitudes set to $\Delta_{\alpha} = 8.5$ and $\Delta_{\beta} = 5$. The broadening is taken to be $\Gamma = 0.5$.

In Fig. 4(c), we consider the case when the orientation of the interface is between [100] and [110] but falls into the window of $\pm 6^{\circ}$ about [100]. In such case, both nonzero-and zero-energy bound states are equally important to the differential conductances and ZBCP is often observed due to zero-energy midgap state. Moreover, when electrons tunnel into the superconductor across the interface, QPs from different bands are coupled. Due to different gap amplitudes on different FSs and finite QP life time, one effective gap amplitude can be generally observed in experiment. In Fig. 4(f), we have used one gap amplitude sign reversal [as done in Fig. 4(a)] to fit the PCARS data [21]. For the best fitting, the effective gap amplitude is taken to be $\overline{\Delta}=6.5$ with broadening being $\Gamma=1.5$, while the sign-change gap amplitude is taken to be $\Delta=5$ with the broadening being $\Gamma=0.01$.

4. summary

In summary, we have derived a phenomenological model to account for the observed tunneling spectroscopy of Fe-pnictide superconductors by taking into the consideration of asymmetric interface scattering between particle and holes. Signatures of anti-phase s^{\pm} -wave pairing in Fe-pnictide superconductors are shown to exhibited as zero-energy surface bound states. In contrast to other pairing symmetries such as d-wave that also supports zero-energy bound states but of a large window of interface orientation for

observing these states, for s^{\pm} -wave, zero-energy bound states can exist only when the orientations of interfaces fall into a small window around $\pm 6^{\circ}$ near the [100] direction. Off the [100] direction, the zero-bias peak disappears and is replaced by two coherent peaks, due to directional dependence of QPs interplaying between different bands. Our results give a unified explanation to the Point-contact Andreev-reflection spectroscopy (PCARS) data in various directions and indicate strongly that current PCARS favor the scenario of s^{\pm} -wave pairing for multi-band Fe-pnictide superconductors .

Finally it is worth noting that PCARS results are very sensitive to the variation and orientation of the micro-crystals. It is indeed a local probe. On the other hand, zero-energy Saint-James cycles is shown to exist only in a small window around $\pm 6^{\circ}$ near the [100] direction. In our modeling, PCARS can only detect the phase difference between the two bands with the same orientation. Moreover, $d_{x^2-y^2}$ -wave symmetry cannot be ruled out if the phase difference between the two bands is $\pi[21]$. The effects of interface disorder may also be important, which will lead to scattering between momentum states along the interface. The PCARS should be more complex than one expects. Only when high-quality single crystal is available and more experiments are performed, one can have a more concrete picture on the pairing symmetry of iron-based superconductors.

Acknowledgments

This work was supported by National Science Council of Taiwan (Grant Nos. 100-2811-M-007-015 and 100-2112-M-007-011-MY3), Hebei Provincial Natural Science Foundation of China (Grant No. A2010001116), and the National Natural Science Foundation of China (Grant No. 10974169). C. S. Liu would like to thank the hospitality of Institute of Applied Physics and Computational Mathematics at Beijingt where some of the work was carried out during his visit. We also acknowledge the support from the National Center for Theoretical Sciences, Taiwan.

- [1] G. R. Stewart, Rev. Mod. Phys. 83, 1589 (2011).
- [2] C. W. Hicks et al., Phys. Rev. Lett. 103, 127003 (2009).
- [3] H.-J. Grafe et al., Phys. Rev. Lett. 101, 047003 (2008).
- [4] K. Hashimoto et al., Phys. Rev. Lett. 102, 017002 (2009).
- [5] Z.-J. Yao, J.-X. Li, and Z. D. Wang, New Journal of Physics 11, 025009 (2009).
- [6] I. I. Mazin, D. J. Singh, M. D. Johannes, and M. H. Du, Phys. Rev. Lett. 101, 057003 (2008).
- [7] F. Wang et al., Phys. Rev. Lett. 102, 047005 (2009).
- [8] F.Wang, H. Zhai, and D.-H. Lee, Phys. Rev. B 81, 184512 (2010).
- [9] C.-T. Chen, C. C. Tsuei, M. B. Ketchen , Z. -A. Ren, and Z. X. Zhao, Nature Physics 6, 260 (2010).
- [10] C.-R. Hu, Phys. Rev. Lett. 72, 1526 (1994).
- [11] Y. Tanaka and S. Kashiwaya, Phys. Rev. Lett. 74, 3451 (1995).
- [12] G. Deutscher, Rev. Mod. Phys. 77, 109 (2005).
- [13] S.-T. Wu and C.-Y. Mou, Phys. Rev. B 66, 012512 (2002).
- [14] S.-T. Wu and C.-Y. Mou, Phys. Rev. B 67, 024503 (2003).
- [15] P. Szabo et al., Phys. Rev. B 79, 012503 (2009).
- [16] M. Tortello et al., Phys. Rev. Lett. 105, 237002 (2010).
- [17] M. Tortello et al., Journal of Superconductivity and Novel Magnetism 22, 553 (2009).
- [18] L. Shan et al., EPL 83, 57004 (2008).

- [19] K. A. Yates et al., Superconductor Science and Technology 21, 092003 (2008).
- [20] X. Lu et al., Superconductor Science and Technology 23, 054009 (2010).
- [21] Y.-L. Wang, L. Shan, L. Fang, P. Cheng, C. Ren, and H.-H. Wen, Superconductor Science and Technology 22, 015018.
- [22] K. A. Yates et al., New Journal of Physics 11, 025015, (2009).
- [23] P. Ghaemi, F. Wang, and A. Vishwanath, Phys. Rev. Lett. 102, 157002 (2009).
- [24] M. A. N. Araujo and P. D. Sacramento, Phys. Rev. B 79, 174529 (2009).
- [25] S. Onari and Y. Tanaka, Phys. Rev. B 79, 174526 (2009).
- [26] A. A. Golubov, A. Brinkman, Y. Tanaka, I. I. Mazin, and O. V. Dolgov, Phys. Rev. Lett. 103, 077003 (2009).
- [27] G. E. Blonder, M. Tinkham, and T. M. Klapwijk, Phys. Rev. B 25, 4515 (1982).
- [28] D. Mou et al., Phys. Rev. Lett. 106, 107001 (2011).
- [29] T. Qian, X.-P. Wang, W.-C. Jin, P. Zhang, P. Richard, G. Xu, X. Dai, Z. Fang, J.-G. Guo, X.-L. Chen, and H. Ding, Phys. Rev. Lett. 106, 187001 (2011).
- [30] Y.-M. Xu et al., arXiv:0905.4467v2.
- [31] D. V. Evtushinsky et al., Phys. Rev. B 79, 054517 (2009).
- [32] D. J. Singh and M.-H. Du, Phys. Rev. Lett. 100, 237003 (2008).
- [33] H. Ding et al., EPL 83, 47001 (2008).
- [34] K. Nakayama et al., Phys. Rev. B 83, 020501 (2011).
- [35] P. G. de Gennes, Superconductivity of Metals and Alloys (Benjamin, New York, 1996).
- [36] J. Bardeen, R. Kummel, A. E. Jacobs, and L. Tewordt, Phys. Rev. 187, 556 (1969).
- [37] A. M. Zagoskin, Quantum Theory of Many-Body Systems: Techniques and Applications (Springer, New York, 1998).
- [38] R. S. Gonnelli, D. Daghero, G. A. Ummarino, V. A. Stepanov, J. Jun, S. M. Kazakov, and J. Karpinski, Phys. Rev. Lett. 89, 247004 (2002).
- [39] A. Brinkman, A. A. Golubov, H. Rogalla, O. V. Dolgov, J. Kortus, Y. Kong, O. Jepsen, and O. K. Andersen, Phys. Rev. B 65, 180517 (2002).
- [40] W. K. Park and L. H. Greene, Rev. Sci. Instrum. 77, 023905 (2006).